An Accurate Algebraic Solution for Moving Source Location Using TDOA and FDOA Measurements

K. C. Ho, *Senior Member, IEEE,* and Wenwei Xu, *Member, IEEE*

***Abstract*—This paper proposes an algebraic solution for the position and velocity of a moving source using the time differences of arrival (TDOAs) and frequency differences of arrival (FDOAs) of a signal received at a number of receivers. The method employs several weighted least-squares minimizations only and does not require initial solution guesses to obtain a location estimate. It does not have the initialization and local convergence problem as in the conventional linear iterative method. The estimated accuracy of the source position and velocity is shown to achieve the Cramér–Rao lower bound for Gaussian TDOA and FDOA noise at moderate noise level before the thresholding effect occurs. Simulations are included to examine the algorithm's performance and compare it with the Taylor-series iterative method.**

***Index Terms*—FDOA, least-squares, passive localization, TDOA.**

I. Introduction

THE problem of passive source location has been of considerable interest for many years. It has found wide applications in many areas including radar, sonar, and wireless communications [1]–[3]. For a stationary emitter, one common technique is to measure the TDOAs of the source signal to a number of spatially separated receivers. Each TDOA defines a hyperbola in which the emitter must lie. The intersection of the hyperbolae gives the source location estimate. When the source is moving, FDOA measurements should be used in addition to TDOAs to estimate accurately the source position and velocity. Numerous techniques are available in literature for stationary source location using TDOAs [5]–[17]. Relatively little work is available, however, for moving source location.

The extended Kalman filter(EKF) [18] is a viable technique to track the location of a moving source. The EKF requires TDOA and FDOA measurements at different times, and an initial transient period is needed before it produces a good source location estimate. The EKF has no optimality properties, and its performance depends on the accuracy of the linearization in the measurement equation [18]. Furthermore, a good initial guess close to the true solution is often required to start the tracking of a target [18].

Determining the source position and velocity from TDOA and FDOA measurements obtained at a single time instant is not a trivial task. This is because the source location is nonlinearly related to TDOA and FDOA measurements. If the source is stationary with known altitude and the FDOAs are from the movement of receivers, Schmidt [19] deduced the location solution for a critically determined situation of one TDOA and one FDOA. Ho and Chan [20] recently derived a closed-form computationally efficient solution for the overdetermined situation. When the source is moving, to the best of our knowledge, no explicit algebraic solution for position and velocity is available in literature.

The most straightforward method to the localization problem is exhaustive search in the solution space. This is very computationally expensive, inefficient, and prohibits real-time processing. A possible alternative is to linearize the TDOA and FDOA equations through Taylor-series expansion [5]. The Taylor-series linearization method requires a proper initial position and velocity guess close to the true solution, and such a good guess may not be easy to obtain in practice. Furthermore, under some circumstances where the source and receiver geometry is not good, the Taylor-series method may fail to converge. For instance, in the simulation performed, the Taylor series method does not converge properly to the true solution if the initial guess has only 1% mean-square error with respect to the true location. Even when the Taylor-series method converges, the solution may not be accurate because 1) convergence to incorrect local minimum may occur, and 2) ignoring the higher order terms in the Taylor-series expansion introduces significant error, as in the case when the measurement curves are approximately parallel. An alternative solution method that does not require initial solution guesses is desirable to perform a better location task.

We will present in this paper a computationally attractive algebraic solution to the source position and velocity using TDOA and FDOA measurements. The proposed solution does not require initial solution guess and involves weighted least-squares minimization only. The proposed solution attains the Cramér–Rao lower bound (CRLB) at moderate noise level when the TDOA noise and FDOA noise are Gaussian. At high noise level, a thresholding effect resulted from the nonlinear nature of the problem occurs, and the estimation accuracy deviates from the CRLB.

The proposed solution method extends the previous work by Chan and Ho [17], [20] that considers the localization of a stationary source only. The proposed method first transforms the TDOA and FDOA equations to a set of linear equations by introducing nuisance parameters. It then applies linear weighted least-squares (LS) to obtain the source position, velocity, and nuisance parameters. Next, the nuisance parameters

Manuscript received March 21, 2002; revised August 11, 2003. The associate editor coordinating the review of this manuscript and approving it for publication was Dr. Vikram Krishnamurthy.

K. C. Ho is with the Department of Electrical and Computer Engineering, University of Missouri, Columbia, MO 65211 USA (e-mail: hod@missouri.edu).

W. Xu was with the Department of Electrical and Computer Engineering, University of Missouri, Columbia, MO 65211 USA. He is now with Legato Video, LLC, Hopewell, NJ 08525 USA.

Digital Object Identifier 10.1109/TSP.2004.831921

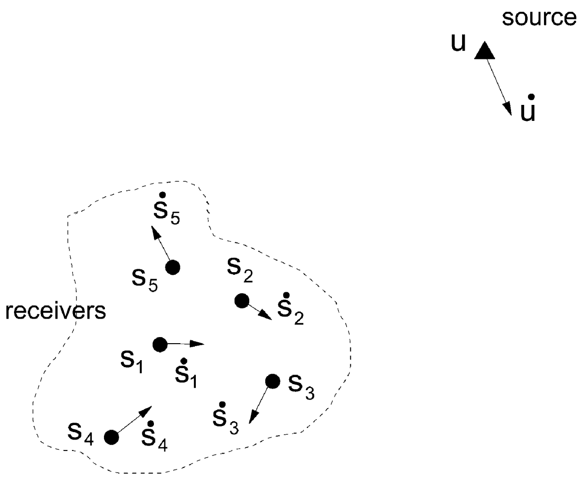

Fig. 1. Geometry for moving source localization.

are eliminated through the use of another linear weighted LS minimization to improve the estimates. This technique falls into the basic framework of the extended invariance principle derived by Stoica *et al.* [21]. The following section presents the derivation of the proposed solution along with the analysis of location accuracy. Section III compares analytically the location accuracy of the proposed estimator to the CRLB for Gaussian measurement noise. Section IV provides some approximations for obtaining the weighting matrices. Section V presents simulations to support the theoretical developments of the proposed estimator and compares them with the Taylor-series linearization method. Finally, conclusions will be drawn in Section VI.

II. Proposed Solution

We consider a three-dimensional (3-D) scenario where an array of M moving sensors is used to determine the position $\mathbf{u} = [x, y, z]^T$ and velocity $\dot{\mathbf{u}} = [\dot{x}, \dot{y}, \dot{z}]^T$ of a moving source using TDOAs and FDOAs, as shown in Fig. 1. The sensor positions $\mathbf{s}_i = [x_i, y_i, z_i]^T$ and velocities $\dot{\mathbf{s}}_i = [\dot{x}_i, \dot{y}_i, \dot{z}_i]^T, i = 1, 2, \ldots, M$ are assumed known. The location problem requires at least $M = 4$ receivers to produce three TDOAs and three FDOAs. This paper focuses on the overdetermined scenario where the number of receivers is larger than 4. We will use the notation $(*)^o$ to denote the true value of the noisy quantity (*).

The proposed solution uses two basic assumptions: A1) The receivers are neither lying on a plane nor on a straight line; A2) the noise standard deviation relative to the true values of the TDOA and FDOA measurements is small. Assumption A1 ensures that the matrix $\mathbf{G}_1$ in the proposed algorithm is nonsingular. It also guarantees that the location solution of the proposed algorithm is unique. There are two possible solutions when the receivers are lying on a plane and an infinite number of solutions when they are lying on a straight line. The solution ambiguity in these cases is due to the location geometry, regardless of the algorithm used to find the solution. Additional knowledge about the source is needed to resolve the ambiguity. When the receivers are lying on a plane, the proposed method described below can be reformulated to obtain a solution, and the details will be reported elsewhere. Assumption A2 simplifies the algorithm development and analysis. It can be satisfied by increasing the observation period in obtaining the TDOA and FDOA measurements.

The distance between the source and the receiver i is

$$r_i^o = |\mathbf{u} - \mathbf{s}_i| = \sqrt{(\mathbf{u} - \mathbf{s}_i)^T(\mathbf{u} - \mathbf{s}_i)}. \tag{1}$$

If the true TDOA of a signal received by the receiver pair i and 1 is t_{i1}^o, and if c is the signal propagation speed, the set of equations that relate the TDOAs and the source position is

$$r_{i1}^o = ct_{i1}^o = r_i^o - r_1^o, \tag{2}$$

where r_{i1}^o is the range difference, and $i = 2, 3, \ldots, M$. Upon rewriting (2) as $r_{i1}^o + r_1^o = r_i^o$, squaring both sides, and substituting (1) for ${r_1^o}^2$ and ${r_i^o}^2$, we arrive at a set of TDOA equations:

$$\begin{aligned} {r_{i1}^o}^2 + 2r_{i1}^o r_1^o = \mathbf{s}_i^T\mathbf{s}_i - \mathbf{s}_1^T\mathbf{s}_1 - 2\left(\mathbf{s}_i - \mathbf{s}_1\right)^T \mathbf{u} \\ i = 2, 3, \ldots, M. \end{aligned} \tag{3}$$

Note that (3) is nonlinear with respect to $\mathbf{u}$ since r_1^o is related to $\mathbf{u}$ through (1). The intersection of the $M-1$ curves in (3) gives the source position estimate.

The TDOA equations only allow the estimation of source position and not velocity. In addition, the TDOA equations alone may not be sufficient to provide enough accuracy to the position estimate. When the FDOA measurements are available, resulting from the relative motion between the source and receivers, we are able to improve the accuracy of position estimate and, at the same time, identify the source velocity.

The time derivative of (1) gives the relationship between the range rate and target location parameters:

$$\dot{r}_i^o = \frac{(\dot{\mathbf{u}} - \dot{\mathbf{s}}_i)^T(\mathbf{u} - \mathbf{s}_i)}{r_i^o}. \tag{4}$$

To make use of FDOAs, we take the time derivative of (3):

$$\begin{aligned} &2\left(\dot{r}_{i1}^o r_{i1}^o + \dot{r}_{i1}^o r_1^o + r_{i1}^o \dot{r}_1^o\right) \\ &\quad = 2\left(\dot{\mathbf{s}}_i^T\mathbf{s}_i - \dot{\mathbf{s}}_1^T\mathbf{s}_1 - (\dot{\mathbf{s}}_i - \dot{\mathbf{s}}_1)^T\mathbf{u} - (\mathbf{s}_i - \mathbf{s}_1)^T\dot{\mathbf{u}}\right) \end{aligned} \tag{5}$$

for $i = 2, 3, \ldots, M$, where $\dot{r}_{i1}^o$ is the range rate differences derived from the FDOAs [22]. When substituting r_1^o and $\dot{r}_1^o$ from (1) and (4), (5) becomes a set of nonlinear equations that relates both TDOAs and FDOAs with the source position $\mathbf{u}$ and velocity $\dot{\mathbf{u}}$. Solving $\mathbf{u}$ and velocity $\dot{\mathbf{u}}$ from the TDOA and FDOA equations is not an easy task.

Let $\mathbf{r} = [r_{21}, r_{31}, \ldots, r_{M1}]^T$ and $\dot{\mathbf{r}} = [\dot{r}_{21}, \dot{r}_{31}, \ldots, \dot{r}_{M1}]^T$ be the vectors of noisy range differences and range rate differences. We will assume that the TDOA and FDOA measurements can be described by the additive noise model as

$$\mathbf{r} = \mathbf{r}^o + c\Delta\mathbf{t}, \quad \dot{\mathbf{r}} = \dot{\mathbf{r}}^o + c\Delta\dot{\mathbf{t}} \tag{6}$$

where $\Delta\mathbf{t} = [\Delta t_{21}, \Delta t_{31}, \ldots, \Delta t_{M1}]^T$, and $\Delta\dot{\mathbf{t}} = [\Delta\dot{t}_{21}, \Delta\dot{t}_{31}, \ldots, \Delta\dot{t}_{M1}]^T$ are the vectors of TDOA and FDOA noise. They are zero mean and have covariance matrix

$$E[[\Delta\mathbf{t}^T \quad \Delta\dot{\mathbf{t}}^T]^T[\Delta\mathbf{t}^T \quad \Delta\dot{\mathbf{t}}^T]] = \frac{1}{c^2}\mathbf{Q}. \tag{7}$$

This noisy measurement model covers many unbiased TDOA and FDOA estimators [23]–[25] and does not impose any distribution on the measurement errors $\Delta\mathbf{t}$ and $\Delta\dot{\mathbf{t}}$. The probability distributions of $\Delta\mathbf{t}$ and $\Delta\dot{\mathbf{t}}$ and their covariance matrix $\mathbf{Q}$ are derived from the specific measuring/estimating technique used to obtain TDOAs and FDOAs. For some estimation methods, such as the maximum likelihood (ML) estimator, $\mathbf{Q}$ approaches the CRLB under Gaussian noise, and it has an explicit form, as shown in [24].

The solution derivation begins by defining an auxiliary vector $\boldsymbol{\theta}_1 = [\mathbf{u}^T, r_1^o, \dot{\mathbf{u}}^T, \dot{r}_1^o]^T$. It contains the unknown source location parameters and two nuisance variables r_1^o and $\dot{r}_1^o$. In the presence of TDOA and FDOA noise, replacing the true range and range rate differences in (3) and (5) by their noisy values results in the equation error vector

$$\boldsymbol{\varepsilon}_1 = \begin{bmatrix} \boldsymbol{\varepsilon}_t \\ \boldsymbol{\varepsilon}_f \end{bmatrix} = \mathbf{h}_1 - \mathbf{G}_1\boldsymbol{\theta}_1 \tag{8}$$

where

$$\mathbf{h}_1 = \begin{bmatrix} r_{21}^2 - \mathbf{s}_2^T\mathbf{s}_2 + \mathbf{s}_1^T\mathbf{s}_1 \\ \vdots \\ r_{M1}^2 - \mathbf{s}_M^T\mathbf{s}_M + \mathbf{s}_1^T\mathbf{s}_1 \\ 2\left(\dot{r}_{21}r_{21} - \dot{\mathbf{s}}_2^T\mathbf{s}_2 + \dot{\mathbf{s}}_1^T\mathbf{s}_1\right) \\ \vdots \\ 2\left(\dot{r}_{M1}r_{M1} - \dot{\mathbf{s}}_M^T\mathbf{s}_M + \dot{\mathbf{s}}_1^T\mathbf{s}_1\right) \end{bmatrix}$$

$$\mathbf{G}_1 = -2\begin{bmatrix} (\mathbf{s}_2-\mathbf{s}_1)^T & r_{21} & \mathbf{0}^T & 0 \\ \vdots & \vdots & \vdots & \vdots \\ (\mathbf{s}_M-\mathbf{s}_1)^T & r_{M1} & \mathbf{0}^T & 0 \\ (\dot{\mathbf{s}}_2-\dot{\mathbf{s}}_1)^T & \dot{r}_{21} & (\mathbf{s}_2-\mathbf{s}_1)^T & r_{21} \\ \vdots & \vdots & \vdots & \vdots \\ (\dot{\mathbf{s}}_M-\dot{\mathbf{s}}_1)^T & \dot{r}_{M1} & (\mathbf{s}_M-\mathbf{s}_1)^T & r_{M1} \end{bmatrix} \tag{9}$$

and $\mathbf{0}$ is a 3×1 column vector of zero. The purpose of introducing the nuisance variables is to make (8) become a set of linear equations with respect to $\boldsymbol{\theta}_1$. The weighted LS solution of $\boldsymbol{\theta}_1$ that minimizes $\boldsymbol{\varepsilon}_1^T\mathbf{W}_1\boldsymbol{\varepsilon}_1$, where $\mathbf{W}_1$ is a positive definite weighting matrix, is [18]

$$\boldsymbol{\theta}_1 = \left(\mathbf{G}_1^T\mathbf{W}_1\mathbf{G}_1\right)^{-1}\mathbf{G}_1^T\mathbf{W}_1\mathbf{h}_1. \tag{10}$$

Condition A1 ensures that the receiver positions will not make $\mathbf{G}_1$ singular, and hence, $(\mathbf{G}_1^T\mathbf{W}_1\mathbf{G}_1)^{-1}$ exists. Since $\mathbf{G}_1$ contains noisy measurements in the fourth and the eighth column, it may be possible that $\mathbf{G}_1$ and, hence, $\mathbf{G}_1\mathbf{W}_1\mathbf{G}_1^T$ become ill-conditioned due to the measurement noise. $\mathbf{G}_1$ is singular if all the TDOA measurements, or all the TDOA and FDOA measurements, are close to zero. Assuming for simplicity that the probability of a measurement becomes zero is p and that the noise in the measurements are independent with one another, then the probabilities for the fourth and the eighth columns to be zero are $p^{2(M-1)}$ and $p^{(M-1)}$, respectively, where M is the number of receivers. Hence, the probability that $\mathbf{G}_1$ becomes ill-conditioned due to measurement noise decreases exponentially as the number of measurements increases. Furthermore, the probability value p decreases as the observation interval in obtaining TDOA and FDOA measurements increases. Although there is no guarantee that $\mathbf{G}_1$ will not be ill-conditioned, the probabilty that it will become ill-conditioned can be made small by increasing the number of receivers and/or the duration of the measurement interval. In our extensive simulation study, we have not encountered any ill-conditioned behavior in $\mathbf{G}_1\mathbf{W}_1\mathbf{G}_1^T$.

There are many possible choices of $\mathbf{W}_1$. The simplest one is identity. When $\mathbf{Q}$ is known, Appendix A gives one particular choice of $\mathbf{W}_1$ that minimizes the parameter variance of $\boldsymbol{\theta}_1$:

$$\mathbf{W}_1 = \mathbf{B}_1^{-T}\mathbf{Q}^{-1}\mathbf{B}_1^{-1} \tag{11}$$

$$\mathbf{B}_1 = \begin{bmatrix} \mathbf{B} & \mathbf{O} \\ \dot{\mathbf{B}} & \mathbf{B} \end{bmatrix}$$
$$\mathbf{B} = 2\mathrm{diag}\{r_2^o, r_3^o, \ldots, r_M^o\}$$
$$\dot{\mathbf{B}} = 2\mathrm{diag}\{\dot{r}_2^o, \dot{r}_3^o, \ldots, \dot{r}_M^o\} \tag{12}$$

and $\mathbf{O}$ is a zero square matrix of appropriate size. Under assumption A2, the second-order noise terms in (33) and (34) tend to zero asymptotically as the measurement noise decreases so that $\boldsymbol{\varepsilon}_1$ is zero mean asymptotically at the true value of $\boldsymbol{\theta}_1$. Hence, from the weighted LS theory [18], $\boldsymbol{\theta}_1$ is asymptotically unbiased. When choosing $\mathbf{W}_1$ in (11) and using A2 so that $\mathbf{G}_1$ is constant, we have

$$\mathrm{cov}(\boldsymbol{\theta}_1) = \left(\mathbf{G}_1^T\mathbf{W}_1\mathbf{G}_1\right)^{-1}. \tag{13}$$

In solving for $\boldsymbol{\theta}_1$, it is assumed that the nuisance variables r_1^o and $\dot{r}_1^o$ are independent of the source position and velocity. They are, in fact, related to $\mathbf{u}$ and $\dot{\mathbf{u}}$, as shown in (1) and (4), by

$$r_1^{o2} = (\mathbf{u}-\mathbf{s}_1)^T(\mathbf{u}-\mathbf{s}_1) \tag{14}$$
$$\dot{r}_1^o r_1^o = (\dot{\mathbf{u}}-\dot{\mathbf{s}}_1)^T(\mathbf{u}-\mathbf{s}_1). \tag{15}$$

The final source position and velocity estimate should minimize the equation errors in (14) and (15) while maintaining as close as possible to the source location values contained in $\boldsymbol{\theta}_1$. Let $\theta_1(i)$ be the ith element of $\boldsymbol{\theta}_1$, $\boldsymbol{\theta}_{1,\mathbf{u}}$ be $[\theta_1(1), \theta_1(2), \theta_1(3)]^T$, and $\boldsymbol{\theta}_{1,\dot{\mathbf{u}}}$ be $[\theta_1(5), \theta_1(6), \theta_1(7)]^T$. To this end, we apply a second-stage process and construct another set of equations

$$\boldsymbol{\varepsilon}_2 = \mathbf{h}_2 - \mathbf{G}_2\boldsymbol{\theta}_2 \tag{16}$$

$$\mathbf{h}_2 = \begin{bmatrix} (\boldsymbol{\theta}_{1,\mathbf{u}}-\mathbf{s}_1)\odot(\boldsymbol{\theta}_{1,\mathbf{u}}-\mathbf{s}_1) \\ \theta_1(4)^2 \\ (\boldsymbol{\theta}_{1,\dot{\mathbf{u}}}-\dot{\mathbf{s}}_1)\odot(\boldsymbol{\theta}_{1,\mathbf{u}}-\mathbf{s}_1) \\ \theta_1(8)\theta_1(4) \end{bmatrix}$$

$$\mathbf{G}_2 = \begin{bmatrix} \mathbf{I} & \mathbf{O} \\ \mathbf{1}^T & \mathbf{0}^T \\ \mathbf{0} & \mathbf{I} \\ \mathbf{0}^T & \mathbf{1}^T \end{bmatrix}$$

$$\boldsymbol{\theta}_2 = \begin{bmatrix} (\mathbf{u}-\mathbf{s}_1)\odot(\mathbf{u}-\mathbf{s}_1) \\ (\dot{\mathbf{u}}-\dot{\mathbf{s}}_1)\odot(\mathbf{u}-\mathbf{s}_1) \end{bmatrix} \tag{17}$$

where $\mathbf{I}$ is a 3×3 identity matrix, $\mathbf{O}$ is a 3×3 matrix of zero, $\mathbf{1}$ is a 3×1 vector of unity, $\mathbf{0}$ is a 3×1 vector of zero, and the symbol $\odot$ represents the Schur product (element-by-element multiplcation). The fourth and the eighth rows are from, respectively, (14) and (15). Minimizing the weighted second norm of $\boldsymbol{\varepsilon}_2$ with a positive definite matrix $\mathbf{W}_2$ yields

$$\boldsymbol{\theta}_2 = \left(\mathbf{G}_2^T\mathbf{W}_2\mathbf{G}_2\right)^{-1}\mathbf{G}_2^T\mathbf{W}_2\mathbf{h}_2. \tag{18}$$

There are many choices for $\mathbf{W}_2$, depending on certain desirable criteria. The simplest choice is identity. Appendix B gives one particular $\mathbf{W}_2$ that minimizes the parameter variance of $\boldsymbol{\theta}_2$:

$$\mathbf{W}_2 = \mathbf{B}_2^{-T}\mathrm{cov}(\boldsymbol{\theta}_1)^{-1}\mathbf{B}_2^{-1} \tag{19}$$

where $\mathbf{B}_2$ is defined in (37). For the particular choice of $\mathbf{W}_2$, Appendix B shows that

$$\mathrm{cov}(\boldsymbol{\theta}_2) = \left(\mathbf{G}_2^T\mathbf{W}_2\mathbf{G}_2\right)^{-1}. \tag{20}$$

From the definition of $\boldsymbol{\theta}_2$ in (17), the final source position estimate $\mathbf{u}$ and velocity estimate $\dot{\mathbf{u}}$ are

$$\mathbf{u} = \mathbf{U}[\sqrt{\theta_2(1)}, \sqrt{\theta_2(2)}, \sqrt{\theta_2(3)}]^T + \mathbf{s}_1 \tag{21}$$

$$\dot{\mathbf{u}} = \mathbf{U}\left[\frac{\theta_2(4)}{\sqrt{\theta_2(1)}}\,\frac{\theta_2(5)}{\sqrt{\theta_2(2)}}\,\frac{\theta_2(6)}{\sqrt{\theta_2(3)}}\right]^T + \dot{\mathbf{s}}_1 \tag{22}$$

where $\mathbf{U} = \mathrm{diag}\{\mathrm{sgn}(\boldsymbol{\theta}_{1,\mathbf{u}} - \mathbf{s}_1)\}$. Note that we keep the sign of the position estimate in the first stage to the final solution in order to remove the sign ambiguity from square root operation. This will ensure that the solution adjustment made by the second stage introduces the least amount of perturbation on the source location estimate in $\boldsymbol{\theta}_1$. Other choices of the signs will result in a solution that increases the cost $\varepsilon_1^T\mathbf{W}_1\varepsilon_1$ in the first stage by a larger amount. A summary of the proposed algorithm is given in Section IV.

We complete the solution derivation by evaluating the bias and variance of the location estimate. The analysis below uses A1 to avoid the singularity of $\mathbf{G}_1$ due to receiver positions and A2 to ignore the higher order error terms appearing in (33) and (34). In addition, the number of receivers is assumed sufficiently large so that the probability that $\mathbf{G}_1$ becomes ill-conditioned due to measurement noise is near zero. Let $\boldsymbol{\theta} = [\mathbf{u}^T, \dot{\mathbf{u}}^T]^T$ be a vector that contains the final source position and velocity estimates. Taking the differential of the vector $\boldsymbol{\theta}_2$ defined in (17) and rearranging yields

$$\Delta\boldsymbol{\theta} = \mathbf{B}_3^{-1}\Delta\boldsymbol{\theta}_2 \tag{23}$$

where

$$\mathbf{B}_3 = \begin{bmatrix} 2\mathrm{diag}\{\mathbf{u}-\mathbf{s}_1\} & \mathbf{O} \\ \mathrm{diag}\{\dot{\mathbf{u}}-\dot{\mathbf{s}}_1\} & \mathrm{diag}\{\mathbf{u}-\mathbf{s}_1\} \end{bmatrix}. \tag{24}$$

Taking expectation of (23) gives the source location bias, and it is related to the bias of $\boldsymbol{\theta}_2$. Under A2, $\boldsymbol{\theta}_1$ is asymptotically unbiased, as explained before (13), and so does $\boldsymbol{\theta}_2$ upon using (36) and (38). As a result, the final location estimate $\boldsymbol{\theta}$ is also asymptotically unbiased in the sense that the biases in $\boldsymbol{\theta}_1$ and $\boldsymbol{\theta}_2$ approach zero asymptotically as the relative measurement error becomes small [Assumption (A2)]. The asymptotically unbiased property of the proposed estimator does not rely on the probability distributions of the TDOA and FDOA measurement noise. Multiplying (23) by its transpose and taking expectation yields

$$\mathrm{cov}(\boldsymbol{\theta}) = \mathbf{B}_3^{-1}\mathrm{cov}(\boldsymbol{\theta}_2)\mathbf{B}_3^{-T}|_{\boldsymbol{\theta}=\boldsymbol{\theta}^o}. \tag{25}$$

In the proposed algorithm, the formulation of the second-stage LS (16) and (17) breaks the 3-D rotational symmetry because of the square and product operations involved in $\mathbf{h}_2$ and $\boldsymbol{\theta}_2$. Hence, a different location solution will result if the coordinate system is rotated by a certain angle. It can be shown, however, from (23) and (25) that the statistical properties of the location solution in terms of asymptotically unbiased behavior and mean-square error remain the same. The asymptotically unbiased property can be shown by taking expectation of (23) after substituting (36) and (38) and realizing that $\boldsymbol{\theta}_1$ remains asymptotically unbiased after coordinate rotation. The invariance property of MSE can be shown through the results in Section III, where the covariance matrix of the proposed location estimate can be expressed in the form given on the right-hand side of (28). Coordinate rotation appears as post-multiplication of the transpose of and pre-multiplication of the orthonormal coordinate rotation matrix in (28). The MSE is the trace of the covariance matrix. Since the trace of $\mathbf{AB}$ is the same as the trace of $\mathbf{BA}$, where $\mathbf{A}$ and $\mathbf{B}$ are square matrices, the coordinate rotation matrices multiply to unity so that the same MSE is obtained in the rotated coordinate system as in the original.

The proposed method has some flavor of the Bancroft algorithm [7], [26] in which LS minimization is applied to the measurement equations. Our approach is different from Bancroft's in that the latter uses pseudo range measurements, computes the position of a user and the GPS clock offset only, does not have nuisance variable, and has only one LS minimization.

The present location task involves the choice of reference receivers. One is for the measurements of TDOAs and FDOAs. The other is for the proposed two-step weighted LS solution method where the nuisance variables r_1^o and $\dot{r}_1^o$ are defined with respect to a reference receiver location. The reference receiver for the measurement and for the solution method can be different.

Let us consider first the reference receiver for the measurements. Denote the TDOA and FDOA measurements using receiver j as the reference by $(d_{ij}, \dot{d}_{ij})$ for $i \neq j, j = 1, 2, \ldots, M$. If the TDOA and FDOA measurements $(d_{ij}, \dot{d}_{ij})$ for a given j are obtained from a joint optimization of all receiver signals such as the maximum likelihood (ML) estimator [23], [29], then they can be formed from the measurements using another receiver k as reference through the equalities

$$d_{ij} = d_{ik} - d_{jk}, \quad \dot{d}_{ij} = \dot{d}_{ik} - \dot{d}_{jk}. \tag{26}$$

Hence, a different choice of reference receivers does not affect the information content from the measurements. For purposes of convenience, the first receiver is chosen as the reference. When the TDOAs and FDOAs are not obtained by jointly optimizing over all receiver signals, the above relationship (26) will not hold. A receiver that has a lower receiver noise and a larger baseline with other receivers should be used as the reference in this case.

Given the set of TDOA and FDOA measurements $(d_{i1}, \dot{d}_{i1})$, we now discuss the choice of reference receiver for the proposed algorithm. Note that (26) can always be used to form the TDOAs and FDOAs with respect to a reference in the proposed algorithm. If $(d_{i1}, \dot{d}_{i1})$ are not obtained by jointly optimizing over all receiver signals, then $(d_{ij}, \dot{d}_{ij})$, formed from (26), will be different from those obtained directly from the received signals using j as the reference.

The choice of different reference receivers does not affect the location accuracy of the proposed method when the weighting matrices (11) and (19) are used. This is because in this case, the location variance (25) resulting from the proposed technique can be reduced to a form that depends on TDOAs and FDOAs only, and no r_1^o and $\dot{r}_1^o$ are involved. This is also supported by the result in the next section, where first the accuracy of the proposed method attains the CRLB under Gaussian noise when the weighting matrices (11) and (19) are used, and second, the CRLB is independent of the choice of reference receiver, as shown in Appendix D. If other weighting matrices are used, the location accuracy will be dependent on the choice of reference receiver. It is not a trivial task to determine beforehand which receiver, as a reference, will give better location accuracy. If additional computation effort is available, we can generate $M-1$ solutions: one for each receiver as the reference. These solutions can then be used in (25) together with (13), (19), and (20) to determine their corresponding expected location variances. The best reference receiver in this case is the one that yields a solution with the minimum expected variance.

The solution given here assumes a simplified ideal environment. In practice, there are many factors that can affect the performance of the proposed algorithm. Some examples include imprecise knowledge of sensor location, multipath, variations in the propagation medium and propagation speed, errors due to asynchronous measurements, and imprecise measurement time.

III. Comparison With the CRLB

The CRLB is the lowest possible variance that an unbiased linear estimator can achieve. It is equal to the inverse of the Fisher matrix defined as [18]

$$\mathbf{J} = E\left[\left(\frac{\partial \ln p(\mathbf{q};\boldsymbol{\theta})}{\partial \boldsymbol{\theta}}\right)^T \left(\frac{\partial \ln p(\mathbf{q};\boldsymbol{\theta})}{\partial \boldsymbol{\theta}}\right)\right]\Bigg|_{\boldsymbol{\theta}=\boldsymbol{\theta}^o} \tag{27}$$

where $\mathbf{q} = [r_{21}, \ldots, r_{M1}, \dot{r}_{21}, \ldots, \dot{r}_{M1}]^T$ is a vector of range and range rate differences from TDOA and FDOA measurements, and $p(\mathbf{q};\boldsymbol{\theta})$ is the probability density function of $\mathbf{q}$ that is parameterized by the vector $\boldsymbol{\theta}$. Assuming an ML TDOA and FDOA estimator so that the asymptotic Gaussian distribution condition holds [18], $p(\mathbf{q};\boldsymbol{\theta})$ is Gaussian with mean $\mathbf{q}^o(\boldsymbol{\theta})$ and covariance matrix $\mathbf{Q}$. After taking natural log and performing differentiation, the CRLB for the underlying problem reduces to

$$\begin{aligned}\mathrm{CRLB}(\boldsymbol{\theta}) &= \mathbf{J}^{-1} \\ &= \left\{\left(\left(\frac{\partial \mathbf{q}^o(\boldsymbol{\theta})}{\partial \boldsymbol{\theta}}\right)^T \mathbf{Q}^{-1} \frac{\partial \mathbf{q}^o(\boldsymbol{\theta})}{\partial \boldsymbol{\theta}}\right)\Bigg|_{\boldsymbol{\theta}=\boldsymbol{\theta}^o}\right\}^{-1}.\end{aligned} \tag{28}$$

Appendix C gives the details on the evaluation of the CRLB from (28).

The location accuracy of the proposed solution method is given in (25). If we use the special choice of the weighting matrices (11) and (19) and substitute the corresponding covariance matrices in (13) and (20), (25) can be expressed as

$$\mathrm{cov}(\boldsymbol{\theta}) = \left((\mathbf{G}_3^T \mathbf{Q}^{-1} \mathbf{G}_3)|_{\boldsymbol{\theta}=\boldsymbol{\theta}^o}\right)^{-1} \tag{29}$$

where

$$\mathbf{G}_3 = \mathbf{B}_1^{-1} \mathbf{G}_1 \mathbf{B}_2^{-1} \mathbf{G}_2 \mathbf{B}_3. \tag{30}$$

Note that (29) has the same form as the CRLB (28). $\mathbf{B}_1$ and $\mathbf{B}_2$ have simple forms, and their inverses can be evaluated symbolically. Substituting the relevant matrices into $\mathbf{G}_3$ and using the results in Appendix C yields, after some straightforward algebraic manipulation

$$\mathbf{G}_3|_{\boldsymbol{\theta}=\boldsymbol{\theta}^o} = \frac{\partial \mathbf{q}^o(\boldsymbol{\theta})}{\partial \boldsymbol{\theta}}\Bigg|_{\boldsymbol{\theta}=\boldsymbol{\theta}^o}. \tag{31}$$

As a result, putting (31) in (29) shows that the estimation accuracy of the proposed estimator attains the CRLB under Gaussian noise when using the weighting matrices (11) and (19).

Appendix D shows that the CRLB is independent of the choice of reference receiver. Hence, for Gaussian noise, the accuracy of the proposed algorithm is also independent of the choice of reference receiver when using the weighting matrices (11) and (19). This is true even when the noise is not Gaussian because (25) can be shown to be independent of r_1 and $\dot{r}_1$.

IV. Implementation

The proposed method requires only weighted LS computation. When using the special weighting matices shown in (11) and (19) to achieve minimum location variance, some approximations are necessary because they contain the true source position and velocity.

The weighting matrix $\mathbf{W}_1$ in (11) depends on $\mathbf{u}$ and $\dot{\mathbf{u}}$ through (1), (4), and (12). For a far-field source moving at a slow speed, the diagonal terms in $\mathbf{B}_1$ dominate, and it becomes diagonal. Since the source is far away from receivers, we have $r_1^o \approx r_2^o \approx \cdots \approx r_M^o$, and $\mathbf{B}_1$ reduces to a scalar multiple of an identity matrix. The effect of weighting matrix is invariant under scaling, and hence, (11) can be approximated by

$$\mathbf{W}_1 = \mathbf{Q}^{-1} \tag{32}$$

and no source position or velocity is needed. On the contrary, if the source is moving relatively fast or the source is close to the receivers, (32) can first be used in (10) to obtain an initial solution $\boldsymbol{\theta}_1$ from which a better weighting matrix $\mathbf{W}_1$ can be formed to produce a better solution.

The weighting matrix $\mathbf{W}_2$ in (19) is dependent on $\mathbf{u}$ and $\dot{\mathbf{u}}$ through (37). At the beginning, we can use the source location solution in $\boldsymbol{\theta}_1$ to form $\mathbf{W}_2$ to produce a solution from which to generate a better $\mathbf{W}_2$ to yield a more accurate solution.

The following summarizes the proposed algorithm when using $\mathbf{W}_1$ and $\mathbf{W}_2$ in (11) and (19).

1) First-Stage Processing:

- Find $\boldsymbol{\theta}_1$ from (10), using $\mathbf{W}_1$ in (32).
- If the source is near-field, repeat the following one to two times:
  — Substitute the source location estimate from $\boldsymbol{\theta}_1$ in (1) and (4), and use (12) and (11) to form $\mathbf{W}_1$.
  — Find $\boldsymbol{\theta}_1$ using (10).

2) Second-Stage Processing:

- Compute $\mathrm{cov}(\boldsymbol{\theta}_1)$ using (13).
- Use the source location estimate from $\boldsymbol{\theta}_1$ in (37) and (19) to form $\mathbf{W}_2$.
- Find $\boldsymbol{\theta}_2$ from (18).
- Apply (21) and (22) to produce $\boldsymbol{\theta}$.
- If the source is near-field, repeat the following one to two times:
  — Use $\boldsymbol{\theta}$ to obtain $\mathbf{B}_2$ defined in (37), where r_1^o and $\dot{r}_1^o$ are computed from (14) and (15).
  — Obtain $\mathbf{W}_2$ using (19).
  — Find $\boldsymbol{\theta}_2$ from (18).
  — Apply (21) and (22) to generate $\boldsymbol{\theta}$.

Repetition is not necessary for far-field sources to achieve CRLB for Gaussian noise. For near-field sources, the proposed algorithm may need repetition to improve accuracy. Repeating the solution computation one to two times is sufficient to yield an accurate solution that reaches the CRLB for Gaussian noise. Additional repetition does not improve accuracy, nor will it degrade accuracy.

Although repetition may be needed for near-field sources, there is no initialization problem. Furthermore, the proposed method always gives the global minimum solution to the quadratic nonlinear source location problem. The purpose of repetition is to reduce the location variance by forming better weighting matrices. The use of the two-step weighted LS minimization technique to solve a general quadratic nonlinear problem is a subject for further study.

The proposed method employs weighted LS where the weighting matrix provides the relative importance of the components of an error vector to be minimized. The weighting matrices derived in Appendix A use small relative measurement error condition A1 so that the second-order error terms can be ignored. To increase the robustness of the algorithm, the weighting matrices should include the second-order error component since they will be nonnegligible when the noise is large. An additional refinement mechanism to mitigate the effect of the nuisance parameters in a large noise environment through a hybrid method with other algorithms is a subject for further study.

The two-step LS minimization and the procedure of plugging an estimate of the weighting matrices into the cost function are reminiscent of some array processing techniques [27], [28] for direction-of-arrival (DOA) estimation. Using an estimate of the weighting matrices was found to have negligible performance degradation [27]. One distinction of the proposed method here is that it introduces nuisance variables in addition to the unknown parameters of interest in the first-stage processing. The second stage refines the solution accuracy using the nuisance parameter values obtained in the first stage. The technique of reparameterization and refinement follows the extended invariance principle proposed by Stoica *et al.* [21].

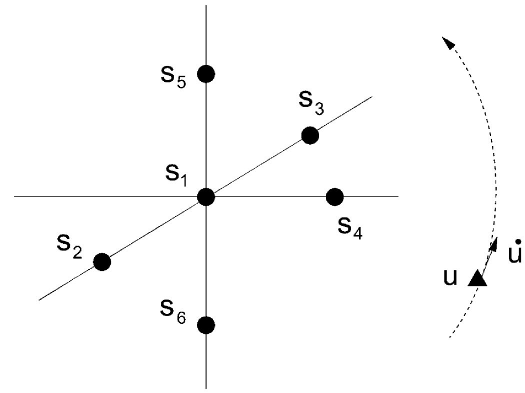

Fig. 2. Location geometry for simulation in Section V-A.

V. SIMULATIONS

This section presents two sets of simulations. The first set investigates the performance of the proposed estimator. The effect of second-stage processing and the inaccurate knowledge of the weighting matrices on the solution accuracy will be examined. The second set compares the mean-square location error of the proposed method with the CRLB and the Taylor-series linearization method. The form of the proposed algorithm described in Section IV was used. In the following simulation scenarios, the unit for the positions is meters, and that for the velocity is meters per second.

A. Investigation of the Proposed Estimator

This subsection examines the accuracy of the proposed estimator in terms of bias μ and standard deviation σ. The TDOA noise and FDOA noise were zero mean Gaussian, and their covariance matrices were $\sigma_d^2\mathbf{R}$ and $\sigma_f^2\mathbf{R}$, where $\mathbf{R}$ is equal to unity in the diagonal elements and 0.5 otherwise [17]. The covariance matrix between TDOA noise and FDOA noise was zero. This choice of $\mathbf{Q}$ corresponds to the ML estimation of TDOAs and FDOAs [24] for equal and uncorrelated receiver noises. The receiver array had six receivers, and they were kept stationary for ease of presentation. The receivers were at $\mathbf{s}_1 = [0,0,0]^T, \mathbf{s}_2 = [400,0,0]^T, \mathbf{s}_3 = [-400,0,0]^T, \mathbf{s}_4 = [0,400,0]^T, \mathbf{s}_5 = [0,0,400]^T, \mathbf{s}_6 = [0,0,-400]^T$. The total number of ensemble runs was 50 000.

In the first simulation, the source was located at a range of $R = 3000$ with an azimuth of $\pi/4$ rad. It was moving along an arc from an elevation angle γ of $-2\pi/9$ rad to $2\pi/9$ rad with an angular velocity of 0.01 rad/s. Fig. 2 shows this source location scenario. The source is far-field since the source range is about ten times the receiver array radius. The TDOA and FDOA noise powers were $\sigma_d^2 = 0.0025/c^2$ and $\sigma_f^2 = 0.000\,25/c^2$. Fig. 3 shows the bias and standard deviation of the source position and velocity estimates of the proposed estimator obtained from only the first-stage processing as well as from the first- and second-stage processing. No repetition for solution computation was applied. In both cases, the bias is relatively small compared with the standard deviation, which verifies that the proposed estimator is asymptotically unbiased when the measurement noise standard devivation relative to the measurement values becomes

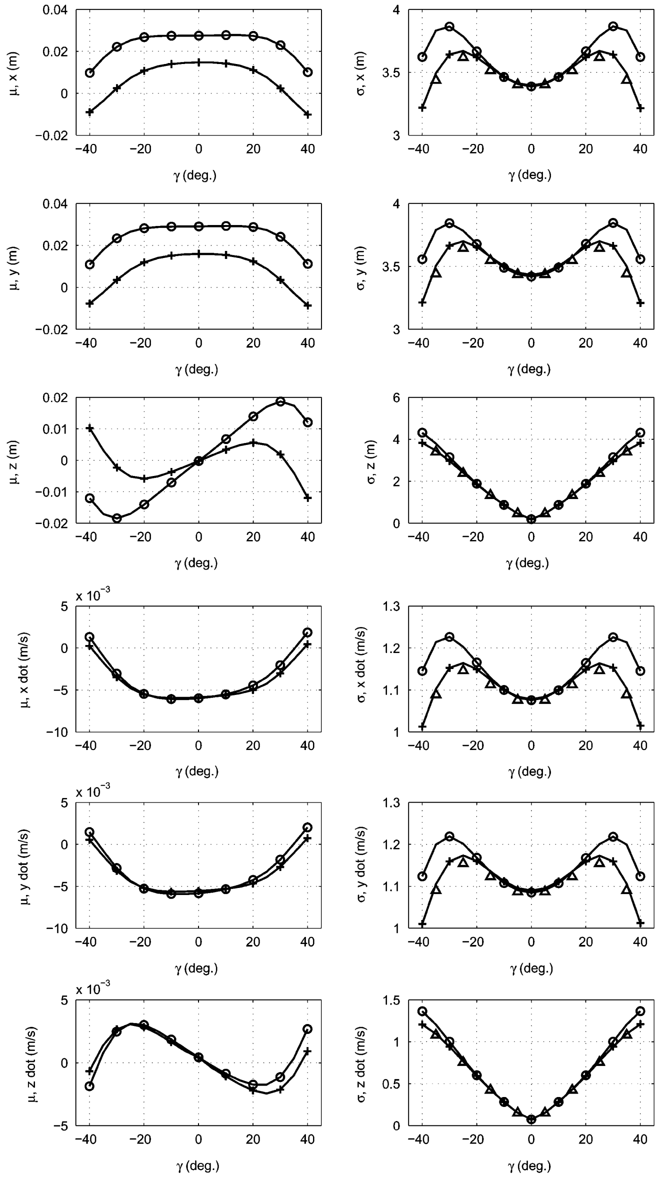

Fig. 3. Bias μ and standard deviation σ for the proposed estimator to localize a far-field source with no repetition. The bias and standard deviation are shown separately for each coordinate component as the elevation angle γ increases. (x, y, z) represents source position and (x dot, y dot, z dot) denotes source velocity. Circle: first-stage processing only. Cross: first- and second-stage processing.

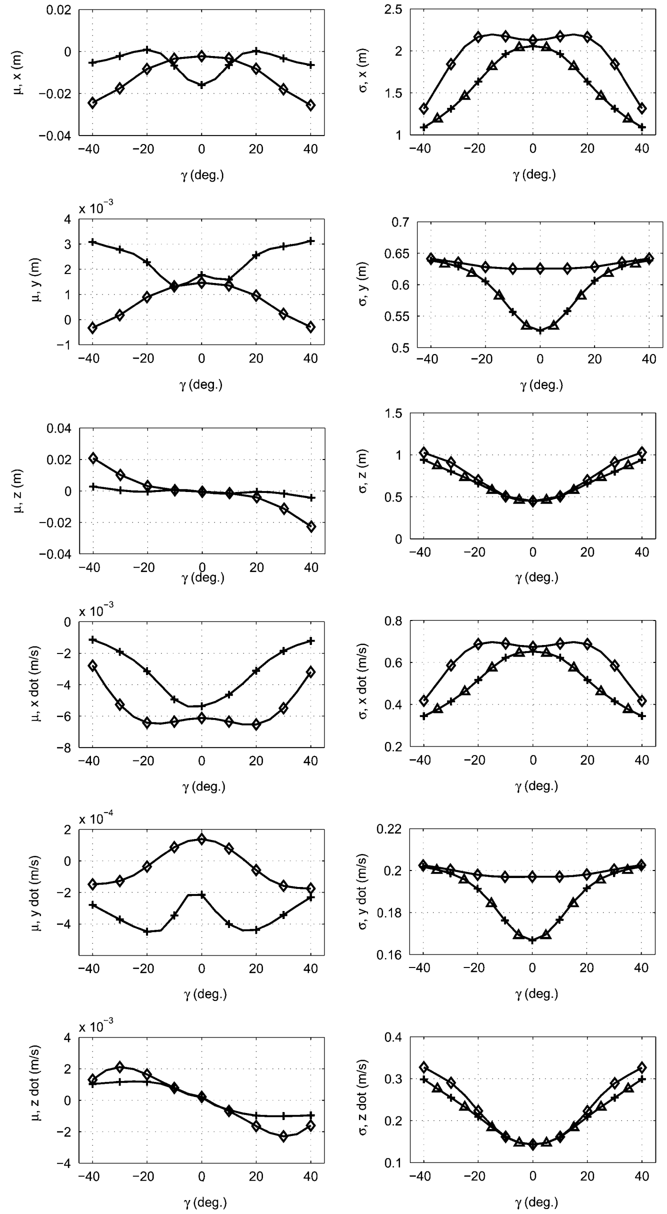

Fig. 4. Bias μ and standard deviation σ for the proposed estimator to localize a near-field source, with zero and one repetition in both the first- and second-stage processing. The bias and standard deviation are shown separately for each coordinate component as the elevation angle γ increases. (x, y, z) represents source position, and (x dot, y dot, z dot) denotes source velocity. Diamond: no repetition. Cross: one repetition.

small. Second-stage processing reduces substantially the position and velocity standard deviations in this simulation experiment, especially when the elevation angle is large. It also reduces the bias in the position estimate.

The CRLBs denoted by the symbol Δ are also shown in the figure. The CRLBs were computed using the expressions in Appendix C. As anticipated from the results in Section III, the performance of the proposed method attains the CRLB in all six unknowns. Reaching the CRLB also corroborates the theoretical understanding that when the source is far-field, the accuracy in source location estimate is insensitive to the inaccurate knowledge of the weighting matrices, and no solution repetition is necessary.

The same set of simulations was repeated for a near-field source, where the source range was changed to $R = 600$, and variance the azimuth was $\pi/18$ rad. The receiver positions, noise distribution, and covariance matrices, as well as the source movement, remained the same as before. The TDOA noise was $0.25/c^2$, and the FDOA noise variance was $0.025/c^2$. Fig. 4 compares the location accuracy when no repetition and one repetition in both the first and second stages was applied in the solution computation. Repetition provides better weighting matrices, thereby giving better results. Repeating solution computation more than once did not improve the results further. In fact, simulations indicate that in most cases, repeating solution computation one to two times is sufficient, and further repetition is not necessary.

Fig. 4 also shows the CRLB for the source location estimate as denoted by the symbol Δ. The accuracy of the proposed solution matches the CRLB very well after one repetition.

TABLE I
POSITIONS AND VELOCITIES OF RECEIVERS

receiver no. i	x_i	y_i	z_i	$\dot{x}_i$	$\dot{y}_i$	$\dot{z}_i$
1	300	100	150	30	-20	20
2	400	150	100	-30	10	20
3	300	500	200	10	-20	10
4	350	200	100	10	20	30
5	-100	-100	-100	-20	10	10

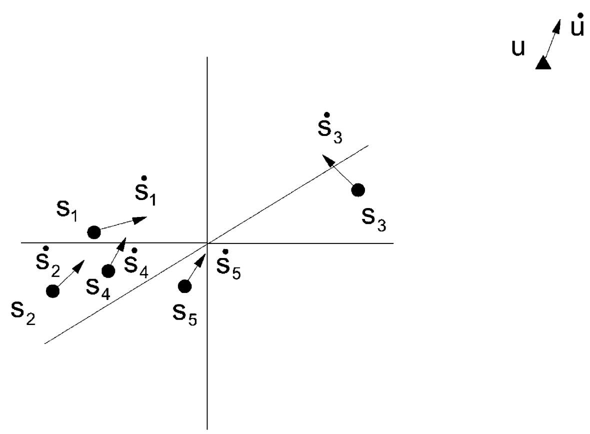

Fig. 5. Location geometry for simulation in Section V-B.

B. Comparison with the Taylor-Series Method and the CRLB

An array of five receivers was chosen, and the positions and velocities of receivers are listed in Table I. The location geometry is shown in Fig. 5. TDOA and FDOA estimates were generated by adding to the true values zero mean Gaussian noise. The covariance matrices of TDOA and FDOA were $\sigma_d^2\mathbf{R}$ and $0.1\sigma_d^2\mathbf{R}$, where $\mathbf{R}$ was set to 1 in the diagonal elements and 0.5 otherwise. The TDOA and FDOA noises were uncorrelated. The number of ensemble runs was 5000.

The true position and velocity of the source were $\mathbf{u} = [2000, 2500, 3000]^T$ and $\dot{\mathbf{u}} = [-20, 15, 40]^T$. Since the source was distant from the receivers and was moving relatively slowly, the required assumptions were satisfied for (32) to hold. Fig. 6 shows the accuracy of position and velocity estimate of the proposed method in terms of root mean-square error (RMSE) as the noise power increases (dashed line). One repetition in both the first and second stages was applied. The estimation accuracy reaches the CRLB at low to moderate noise level and deviates from the CRLB when the noise level is large. The thresholding effect is due to the nonlinear nature of an estimation problem [24], [30]. This thresholding phenomenon in the proposed method is a consequence of ignoring the second-order error terms in deriving the solution, which is not valid when the noise is large. When there is no repetition in the solution computation, the accuracy in both position and velocity is only about 1.1 times higher than the CRLB before the thresholding effect occurs. The result from the Taylor-series linearization method [5] is also given. The method uses truncated Taylor-series expansion to linearize the TDOA and FDOA equations and solves the solution iteratively. The Taylor-series method can be considered to be an iterative technique to solve the ML solution in Gaussian noise.

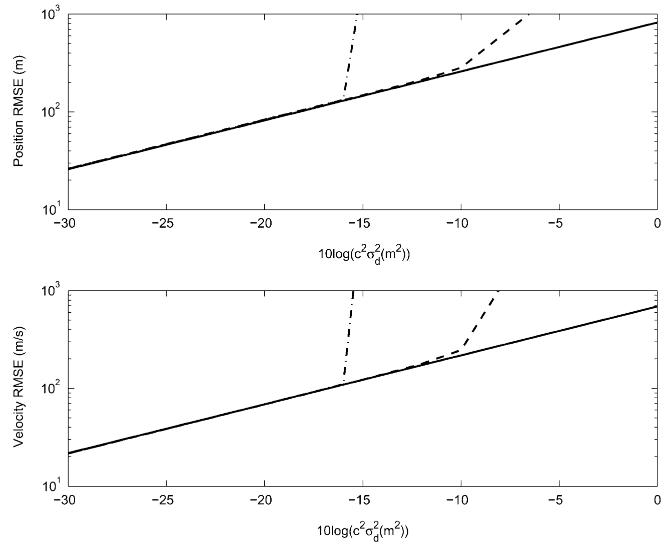

Fig. 6. Comparison of root mean-square error (RMSE) of the proposed method with the Taylor-series linearization method and the CRLB, far-field source and one repetition. The accuracy is shown in log scale as the noise power increases. Dashed: proposed method. Dash-dot: Taylor-series method initialized at true location with Gaussian noise having power twice the CRLB. Solid: CRLB.

We first try the Taylor-series method when the initial guess is set randomly around the true location by adding independent zero mean Gaussian noise that generates 1% mean-square error (MSE) in each position and velocity components. Even with this small amount of error, the Taylor-series method fails to converge to the true solution and gives an RMSE for both position and velocity on the order of 10^6, regardless of the amount of measurement noise. When the initial guess is set to the true solution added with independent zero mean Gaussian noise that has a variance twice the CRLB in each position and velocity components, the Taylor-series method converges at low noise level (dash-dot line). At least three iterations are necessary to reach a solution. Both the Taylor-series method and the proposed estimator yield the same accuracy by attaining the CRLB at low noise level. Although converging, the Taylor-series method deviates from the CRLB and gives an inaccurate solution at a noise power that is about 6 dB lower than the proposed technique. The proposed estimator, in fact, achieves optimum performance by reaching the CRLB (solid line) at a moderate noise level. This corroborates the theoretical comparison between the accuracy of the proposed estimator and the CRLB.

Fig. 7 depicts the results for a near-field source at $\mathbf{u} = [300, 325, 275]^T$ with a velocity of $\dot{\mathbf{u}} = [-20, 15, 40]^T$. One repetition was applied in the first and second stage of solution computation. Again, the Taylor-series method fails to converge when initialized with 1.

The simulation so far uses Gaussian TDOA and FDOA noise. In order to obtain some insight on the performance of the proposed method for non-Gaussian noise, Fig. 8 gives the location accuracy for zero-mean Laplacian-distributed TDOA and FDOA noise. The same noise covariance matrix $\mathbf{Q}$ was used.

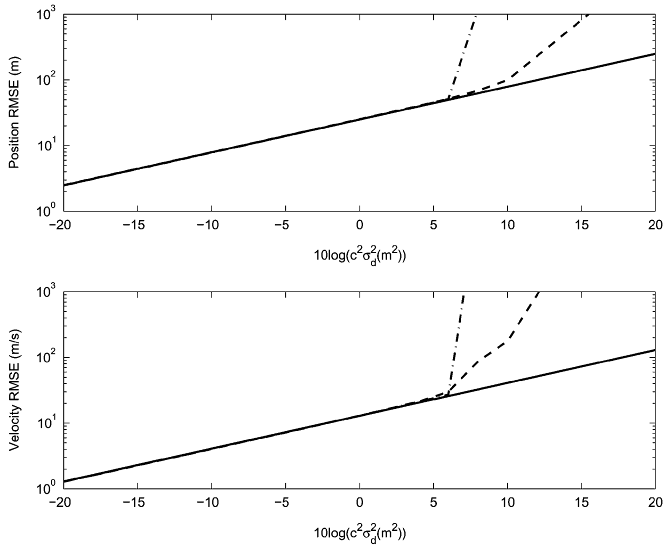

Fig. 7. Comparison of root mean-square error (RMSE) of the proposed method with the Taylor-series linearization method and the CRLB, near-field source, and one repetition. The accuracy is shown in log scale as the noise power increases. Dashed: proposed method. Dash-dot: Taylor-series method initialized at true location with Gaussian noise having power twice the CRLB. Solid: CRLB.

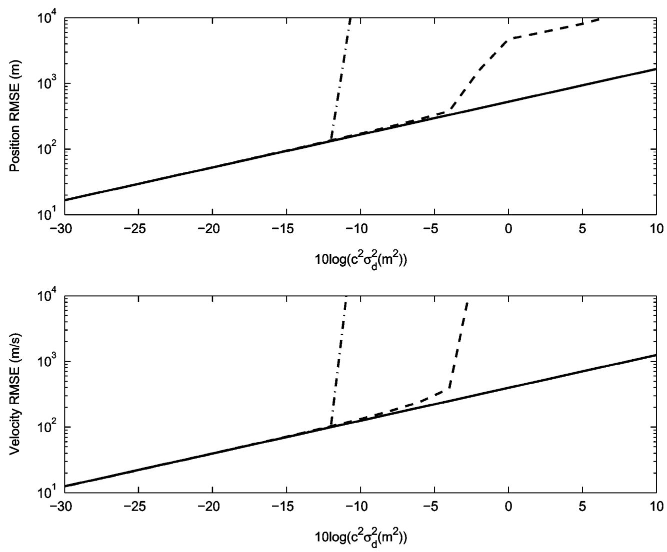

Fig. 8. Comparison of root mean-square error (RMSE) of the proposed method with the Taylor-series linearization method and the theoretical accuracy, Laplacian distributed noise and one repetition. Dashed: proposed method. Dash-dot: Taylor-series method initialized at true location with Gaussian noise having power twice the theoretical minimum variance from (25). Solid: theoretial variance from (25).

The source position and velocity were $\mathbf{u} = [1000, 2000, 1500]^T$ and $\dot{\mathbf{u}} = [-20, 15, 40]^T$. One repetition in the two stages was applied to improve accuracy. The solid curve is from the theoretical covariance formula (25) of the proposed location method, the dashed curve is the result of the proposed method, and the dash-dot curve is the Taylor-series method initialized at the true location added with independent zero mean Gaussian noise that has a power equal to twice the theoretical variance in (25) in each position as well as velocity components. It is clear that the proposed method outperforms the Taylor-series method, and the theoretical formula predicts the performance well. We would expect that since the noise is not Gaussian, the proposed method will not achieve the CRLB.

VI. Conclusion

This paper developed an alegbraic solution for estimating the position and velocity of a moving source based on TDOA and FDOA measurements from an array of receivers. The solution method introduces nuisance variables that allow the source location to be solved efficiently and subsequently exploits the estimated nuisance parameter values to improve the source location estimates. The proposed technique employs weighted least-squares minimization only and is computationally attractive. It does not have convergence and initialization problems, as in the Taylor-series iterative method. The estimation accuracy of the proposed method is shown to achieve the CRLB for Gaussian noise before the thresholding effect occurs.

Appendix A
Weighting Matrix $\mathbf{W}_1$ for Minimum Parameter Variance of $\boldsymbol{\theta}_1$

The weighting matrix that minimizes the parameter variance of $\boldsymbol{\theta}_1$ is $E[\varepsilon_1 \varepsilon_1^T|_{\boldsymbol{\theta}_1^o}]^{-1}$ [18], where $\boldsymbol{\theta}_1^o$ is the true value of $\boldsymbol{\theta}_1$. To find $\mathbf{W}_1$, we will first evaluate the TDOA and FDOA equation error vectors $\boldsymbol{\varepsilon}_t$ and $\boldsymbol{\varepsilon}_f$ separately. Upon putting $\boldsymbol{\theta}_1^o$ into the first half of (8) and expressing r_{i1} as $r_{i1}^o + c\Delta t_{i1}$ from the noise model (6), we have, after using (3)

$$\varepsilon_t|_{\boldsymbol{\theta}_1^o} = c\mathbf{B}\Delta\mathbf{t} + c^2 \Delta\mathbf{t} \odot \Delta\mathbf{t} \approx c\mathbf{B}\Delta\mathbf{t} \tag{33}$$

where $\mathbf{B} = 2\text{diag}\{r_2^o, r_3^o, \ldots, r_M^o\}$ is a diagonal matrix whose elements are the true ranges between the source and receivers, and $\odot$ represents the Schur product (element by element multiplication). We have used the assumption A2) $r_i^o \gg c\Delta t_{i1}$ in (33) to simplify ε_t. Similarly, using the measurement model (6) and evaluating the second half of (8) at the true solution $\boldsymbol{\theta}_1^o$ yields, after using (5)

$$\begin{aligned}\boldsymbol{\varepsilon}_f|_{\boldsymbol{\theta}_1^o} &= c(\dot{\mathbf{B}}\Delta\mathbf{t} + \mathbf{B}\Delta\dot{\mathbf{t}}) + 2c^2\Delta\mathbf{t} \odot \Delta\dot{\mathbf{t}} \\ &\approx c(\dot{\mathbf{B}}\Delta\mathbf{t} + \mathbf{B}\Delta\dot{\mathbf{t}}) \end{aligned} \tag{34}$$

where $\dot{\mathbf{B}} = 2\text{diag}\{\dot{r}_2^o, \dot{r}_3^o, \ldots, \dot{r}_M^o\}$ is a diagonal matrix whose elements are the true range rates between the source and receivers. In (34), we have used the assumption A2), where $\dot{r}_i^o \gg c\Delta\dot{t}_{i1}$ and $r_i^o \gg c\Delta t_{i1}$ for simplification. From (33) and (34)

$$\boldsymbol{\varepsilon}_1|_{\boldsymbol{\theta}_1^o} = c\mathbf{B}_1 \begin{bmatrix} \Delta\mathbf{t} \\ \Delta\dot{\mathbf{t}} \end{bmatrix} \tag{35}$$

where $\mathbf{B}_1$ is given in (12). Multiplying (35) with its transpose, taking expectation and inverse yields (11).

Appendix B
Weighting Matrix $\mathbf{W}_2$ for Minimum Parameter Variance of $\boldsymbol{\theta}_2$

The $\mathbf{W}_2$ that gives the minimum parameter variance of $\boldsymbol{\theta}_2$ is $E[\varepsilon_2 \varepsilon_2^T|_{\boldsymbol{\theta}_2^o}]^{-1}$ [18], where $\boldsymbol{\theta}_2^o$ is the true value of $\boldsymbol{\theta}_2$. When putting $\boldsymbol{\theta}_1 = \boldsymbol{\theta}_1^o + \Delta\boldsymbol{\theta}_1$, where $\Delta\boldsymbol{\theta}_1$ is the estimation noise of $\boldsymbol{\theta}_1$, it is straightforward to deduce from (16) that

$$\boldsymbol{\varepsilon}_2|_{\boldsymbol{\theta}_2=\boldsymbol{\theta}_2^o} = \Delta\mathbf{h}_2 \approx \mathbf{B}_2\Delta\boldsymbol{\theta}_1 \tag{36}$$

where

$$\mathbf{B}_2 = \begin{bmatrix} 2\text{diag}\{\mathbf{u}-\mathbf{s}_1\} & \mathbf{0} & \mathbf{O} & \mathbf{0} \\ \mathbf{0}^T & 2r_1^o & \mathbf{0}^T & 0 \\ \text{diag}\{\dot{\mathbf{u}}-\dot{\mathbf{s}}_1\} & \mathbf{0} & \text{diag}\{\mathbf{u}-\mathbf{s}_1\} & \mathbf{0} \\ \mathbf{0}^T & \dot{r}_1^o & \mathbf{0}^T & r_1^o \end{bmatrix} \tag{37}$$

and second-order error terms have been ignored. Hence, multiplying (36) with its transpose, taking expectation and inverse gives the weighting matrix (19).

Note that $\boldsymbol{\theta}_2^o = (\mathbf{G}_2^T\mathbf{W}_2\mathbf{G}_2)^{-1}\mathbf{G}_2^T\mathbf{W}_2\mathbf{G}_2\boldsymbol{\theta}_2^o = (\mathbf{G}_2^T\mathbf{W}_2\mathbf{G}_2)^{-1}\mathbf{G}_2^T\mathbf{W}_2\mathbf{h}_2^o$. Subtracting both sides of (18) by $\boldsymbol{\theta}_2^o$ yields

$$\Delta\boldsymbol{\theta}_2 = \left(\mathbf{G}_2^T\mathbf{W}_2\mathbf{G}_2\right)^{-1}\mathbf{G}_2^T\mathbf{W}_2\Delta\mathbf{h}_2. \tag{38}$$

The matrix $\mathbf{G}_2$ is constant. Since from (36) $\mathbf{W}_2^{-1} = E[\Delta\mathbf{h}_2\Delta\mathbf{h}_2^T]$, post-multiplying (38) by its transpose and taking expectation gives the covariance matrix of $\boldsymbol{\theta}_2$, as shown in (20).

APPENDIX C
DERIVATION OF THE CRLB FOR THE SOURCE POSITION AND VELOCITY

Let $\mathbf{r}^o(\boldsymbol{\theta}) = [r_{21}^o(\boldsymbol{\theta})\ldots r_{M1}^o(\boldsymbol{\theta})]^T$ and $\dot{\mathbf{r}}^o(\boldsymbol{\theta}) = [\dot{r}_{21}^o(\boldsymbol{\theta})\ldots;\dot{r}_{M1}^o(\boldsymbol{\theta})]^T$. Then, $\mathbf{q}^o(\boldsymbol{\theta}) = [\mathbf{r}^{oT}(\boldsymbol{\theta}), \dot{\mathbf{r}}^{oT}(\boldsymbol{\theta})]^T$, and $\partial\mathbf{q}^o(\boldsymbol{\theta})/\partial\boldsymbol{\theta}$ in (28) can be expressed as

$$\frac{\partial\mathbf{q}^o(\boldsymbol{\theta})}{\partial\boldsymbol{\theta}} = \begin{bmatrix} \frac{\partial\mathbf{r}^o(\boldsymbol{\theta})}{\partial\mathbf{u}} & \frac{\partial\mathbf{r}^o(\boldsymbol{\theta})}{\partial\dot{\mathbf{u}}} \\ \frac{\partial\dot{\mathbf{r}}^o(\boldsymbol{\theta})}{\partial\mathbf{u}} & \frac{\partial\dot{\mathbf{r}}^o(\boldsymbol{\theta})}{\partial\dot{\mathbf{u}}} \end{bmatrix}. \tag{39}$$

We have from (1)

$$r_{i1}^o(\boldsymbol{\theta}) = r_i^o(\boldsymbol{\theta}) - r_1^o(\boldsymbol{\theta}) = |\mathbf{u}-\mathbf{s}_i| - |\mathbf{u}-\mathbf{s}_1| \tag{40}$$

and from (4)

$$\begin{aligned}\dot{r}_{i1}^o(\boldsymbol{\theta}) &= \dot{r}_i^o(\boldsymbol{\theta}) - \dot{r}_1^o(\boldsymbol{\theta}) \\ &= \frac{(\dot{\mathbf{u}}-\dot{\mathbf{s}}_i)^T(\mathbf{u}-\mathbf{s}_i)}{r_i^o(\boldsymbol{\theta})} - \frac{(\dot{\mathbf{u}}-\dot{\mathbf{s}}_1)^T(\mathbf{u}-\mathbf{s}_1)}{r_1^o(\boldsymbol{\theta})}.\end{aligned} \tag{41}$$

Performing the partial derivatives of $r_{i1}^o(\boldsymbol{\theta})$ and $\dot{r}_{i1}^o(\boldsymbol{\theta})$ with respect to $\mathbf{u}$ and $\dot{\mathbf{u}}$ yields (42)–(45), shown at the bottom of the page.

APPENDIX D
PROOF THAT THE CRLB IS INDEPENDENT OF THE CHOICE OF REFERENCE RECEIVER

Let $\mathbf{q}_j = [r_{1,j},\ldots,r_{j-1,j},r_{j+1,j},\ldots,r_{M,j},\dot{r}_{1,j},\ldots,\dot{r}_{j-1,j},\dot{r}_{j+1,j},\ldots,\dot{r}_{M,j}]^T$ be the collection of range and range rate differences from TDOA and FDOA measurements when using receiver j as the reference, where $j = 1,2,\ldots,M$. Since $r_{i,j} = r_i - r_j$ and $\dot{r}_{i,j} = \dot{r}_i - \dot{r}_j$, we can define the sparse matrix

$$\mathbf{P}_j = \begin{bmatrix} \tilde{\mathbf{P}}_j & \mathbf{O} \\ \mathbf{O} & \tilde{\mathbf{P}}_j \end{bmatrix}$$

$$\tilde{\mathbf{P}}_j = \begin{cases} \mathbf{P}_{m,j-1} = -1, & m = 1,2,\ldots,M-1 \\ \mathbf{P}_{m,m-1} = 1, & m = 2,3,\ldots,j-1 \\ \mathbf{P}_{m,m} = 1, & m = j,j+1,\ldots,M-1 \end{cases} \tag{46}$$

such that

$$\mathbf{q}_j = \mathbf{P}_j\mathbf{q}_1 \tag{47}$$

where $\tilde{\mathbf{P}}_j$ is a $(M-1)\times(M-1)$ square matrix, and $\mathbf{O}$ is a $M-1$ square matrix of zeros. The sparse matrix $\mathbf{P}_j$ is full rank. Correspondingly, the covariance matrix of $\mathbf{q}_j$ is

$$\mathbf{Q}_j = \mathbf{P}_j\mathbf{Q}_1\mathbf{P}_j^T. \tag{48}$$

The CRLB of $\boldsymbol{\theta}$ when using receiver j as the reference is, when substituting (47) and (48)

$$\begin{aligned}\text{CRLB}(\boldsymbol{\theta})_j &= \left\{\left(\left(\frac{\partial\mathbf{q}_j^o(\boldsymbol{\theta})}{\partial\boldsymbol{\theta}}\right)^T\mathbf{Q}_j^{-1}\frac{\partial\mathbf{q}_j^o(\boldsymbol{\theta})}{\partial\boldsymbol{\theta}}\right)\bigg|_{\boldsymbol{\theta}=\boldsymbol{\theta}^o}\right\}^{-1} \\ &= \left\{\left(\left(\frac{\partial\mathbf{q}_1^o(\boldsymbol{\theta})}{\partial\boldsymbol{\theta}}\right)^T\mathbf{P}_j^T\right.\right. \\ &\quad\left.\left.\times\ \left(\mathbf{P}_j\mathbf{Q}_1\mathbf{P}_j^T\right)^{-1}\mathbf{P}_j\frac{\partial\mathbf{q}_1^o(\boldsymbol{\theta})}{\partial\boldsymbol{\theta}}\right)\bigg|_{\boldsymbol{\theta}=\boldsymbol{\theta}^o}\right\}^{-1} \\ &= \left\{\left(\left(\frac{\partial\mathbf{q}_1^o(\boldsymbol{\theta})}{\partial\boldsymbol{\theta}}\right)^T\mathbf{Q}_1^{-1}\frac{\partial\mathbf{q}_1^o(\boldsymbol{\theta})}{\partial\boldsymbol{\theta}}\right)\bigg|_{\boldsymbol{\theta}=\boldsymbol{\theta}^o}\right\}^{-1} \\ &= \text{CRLB}(\boldsymbol{\theta})_1 \quad \forall j = 2,3,\ldots,M-1.\end{aligned} \tag{49}$$

$$\left(\frac{\partial\mathbf{r}^o(\boldsymbol{\theta})}{\partial\mathbf{u}}\right) = \begin{bmatrix} \frac{(\mathbf{u}-\mathbf{s}_2)^T}{r_2^o(\boldsymbol{\theta})} - \frac{(\mathbf{u}-\mathbf{s}_1)^T}{r_1^o(\boldsymbol{\theta})} \\ \vdots \\ \frac{(\mathbf{u}-\mathbf{s}_M)^T}{r_M^o(\boldsymbol{\theta})} - \frac{(\mathbf{u}-\mathbf{s}_1)^T}{r_1^o(\boldsymbol{\theta})} \end{bmatrix}_{(M-1)\times 3} \tag{42}$$

$$\left(\frac{\partial\mathbf{r}^o(\boldsymbol{\theta})}{\partial\dot{\mathbf{u}}}\right) = \mathbf{O}_{(M-1)\times 3} \tag{43}$$

$$\left(\frac{\partial\dot{\mathbf{r}}^o(\boldsymbol{\theta})}{\partial\mathbf{u}}\right) = -\begin{bmatrix} \frac{(\mathbf{u}-\mathbf{s}_2)^T\dot{r}_2^o(\boldsymbol{\theta})}{r_2^{o2}(\boldsymbol{\theta})} - \frac{(\mathbf{u}-\mathbf{s}_1)^T\dot{r}_1^o(\boldsymbol{\theta})}{r_1^{o2}(\boldsymbol{\theta})} - \frac{(\dot{\mathbf{u}}-\dot{\mathbf{s}}_2)^T}{r_2^o(\boldsymbol{\theta})} + \frac{(\dot{\mathbf{u}}-\dot{\mathbf{s}}_1)^T}{r_1^o(\boldsymbol{\theta})} \\ \vdots \\ \frac{(\mathbf{u}-\mathbf{s}_M)^T\dot{r}_M^o(\boldsymbol{\theta})}{r_M^{o2}(\boldsymbol{\theta})} - \frac{(\mathbf{u}-\mathbf{s}_1)^T\dot{r}_1^o(\boldsymbol{\theta})}{r_1^{o2}(\boldsymbol{\theta})} - \frac{(\dot{\mathbf{u}}-\dot{\mathbf{s}}_M)}{r_M^o(\boldsymbol{\theta})} + \frac{(\dot{\mathbf{u}}-\dot{\mathbf{s}}_1)^T}{r_1^o(\boldsymbol{\theta})} \end{bmatrix}_{(M-1)\times 3} \tag{44}$$

$$\frac{\partial\dot{\mathbf{r}}^o(\boldsymbol{\theta})}{\partial\dot{\mathbf{u}}} = \frac{\partial\mathbf{r}^o(\boldsymbol{\theta})}{\partial\mathbf{u}}. \tag{45}$$

Hence, the CRLB of $\boldsymbol{\theta}$ is independent of the choice of reference receiver.

ACKNOWLEDGMENT

The authors would like to thank the reviewers for their valuable comments, suggestions, and corrections, which has greatly improved the quality of the paper.

REFERENCES

[1] G. C. Carter, "Time delay estimation for passive sonar signal processing," *IEEE Trans. Acoust., Speech, Signal Processing*, vol. ASSP-29, pp. 462–470, June 1981.

[2] E. Weinstein, "Optimal source localization and tracking from passive array measurements," *IEEE Trans. Acoust., Speech, Signal Processing*, vol. ASSP-30, pp. 69–76, Feb. 1982.

[3] T. S. Rappaport, J. H. Reed, and B. D. Woerner, "Position location using wireless communications on highways of the future," *IEEE Commun. Mag.*, vol. 14, pp. 33–41, Oct. 1996.

[4] J. J. Caffery and G. L. Stuber, "Overview of radiolocation in CDMA cellular systems," *IEEE Commun. Mag.*, vol. 16, pp. 38–45, Apr. 1998.

[5] W. H. Foy, "Position-location solution by Taylor-series estimation," *IEEE Trans. Aerosp. Elect. Syst.*, vol. AES-12, pp. 187–194, Mar. 1976.

[6] D. J. Torrieri, "Statistical theory of passive location systems," *IEEE Trans. Aerosp. Elect. Syst.*, vol. AES-20, pp. 183–198, Mar. 1984.

[7] S. Bancroft, "An algebraic solution of the GPS equations," *IEEE Trans. Aerosp. Elect. Syst.*, vol. AES-21, pp. 224–232, Jan. 1985.

[8] B. Friedlander, "A passive localization algorithm and its accuracy analysis," *IEEE J. Ocean Eng.*, vol. OE-12, pp. 234–245, Jan. 1987.

[9] J. O. Smith and J. S. Abel, "Closed-form least-squares source location estimation from range-difference measurements," *IEEE Trans. Acoust., Speech, Signal Processing*, vol. ASSP-35, pp. 1661–1669, Dec. 1987.

[10] T. T. Ha and R. C. Robertson, "Geostationary satellite navigation systems," *IEEE Trans. Aerosp. Elect. Syst.*, vol. AES-23, pp. 247–254, Mar. 1987.

[11] L. O. Krause, "A direct solution to GPS-type navigation equations," *IEEE Trans. Aerosp. Elect. Syst.*, vol. AES-23, pp. 224–232, Mar. 1987.

[12] H. C. Schau and A. Z. Robinson, "Passive source localization employing intersecting spherical surfaces from time-of-arrival differences," *IEEE Trans. Acoust., Speech, Signal Processing*, vol. ASSP-35, pp. 1223–1225, Aug. 1987.

[13] W. W. Smith Jr. and P. G. Steffes, "Time delay techniques for satellite interference location system," *IEEE Trans. Aerosp. Elect. Syst.*, vol. 25, pp. 224–230, Mar. 1989.

[14] J. S. Abel, "A divide and conquer approach to least-squares estimation," *IEEE Trans. Aerosp. Elect. Syst.*, vol. 26, pp. 423–427, Mar. 1990.

[15] B. T. Fang, "Simple solutions for hyperbolic and related position fixes," *IEEE Trans. Aerosp. Elect. Syst.*, vol. 26, pp. 748–753, Sept. 1990.

[16] J. S. Abel, "Existence and uniqueness of GPS solutions," *IEEE Trans. Aerosp. Elect. Syst.*, vol. 27, pp. 952–956, Nov. 1991.

[17] Y. T. Chan and K. C. Ho, "A simple and efficient estimator for hyperbolic location," *IEEE Trans. Signal Processing*, vol. 42, pp. 1905–1915, Aug. 1994.

[18] S. M. Kay, *Fundamentals of Statistical Signal Processing, Estimation Theory*. Englewood Cliffs, NJ: Prentice-Hall, 1993.

[19] R. O. Schmidt, "An Algorithm for Two-Receiver TDOA/FDOA Emitter Location," ESL, Inc., Tech. Memo. TM-1229, May 1980.

[20] K. C. Ho and Y. T. Chan, "Geolocation of a known altitude object from TDOA and FDOA measurements," *IEEE Trans. Aerosp. Elect. Syst.*, vol. 33, pp. 770–782, July 1997.

[21] P. Stoica and T. Soderstrom, "On reparametrization of loss functions used in estimation and the invariance principle," *Signal Process.*, vol. 17, no. 4, pp. 383–387, Aug. 1989.

[22] P. C. Chestnut, "Emitter location accuracy using TDOA and differential doppler," *IEEE Trans. Aerosp. Elect. Syst.*, vol. AES-18, pp. 214–218, Mar. 1982.

[23] C. H. Knapp and G. C. Carter, "Estimation of time delay in the presence of source or receiver motion," *J. Acoust. Soc. Amer.*, vol. 61, no. 6, pp. 1545–1549, June 1977.

[24] E. Weinstein and D. Kletter, "Delay and Doppler estimation by time-space partition of the array data," *IEEE Trans. Aerosp. Elect. Syst.*, vol. ASSP-31, pp. 1523–1535, Dec. 1983.

[25] K. C. Ho and Y. T. Chan, "Optimum discrete wavelet scaling and its application to delay and Doppler estimation," *IEEE Trans. Signal Processing*, vol. 46, pp. 2285–2290, Sept. 1998.

[26] G. Strang and K. Borre, *Linear Algebra, Geodesy and GPS*. Cambridge, MA: Wellesley-Cambridge Press, 1997.

[27] P. Stoica and K. Sharman, "Maximum likelihood methods for direction of arrival estimation," *IEEE Trans. Acoust., Speech, Signal Processing*, vol. 38, pp. 1132–1143, July 1990.

[28] J. Li, B. Halder, P. Stoica, and M. Viberg, "Computationally efficient angle estimation for signals with known waveforms," *IEEE Trans. Signal Processing*, vol. 43, pp. 2154–2163, Sept. 1995.

[29] G. C. Carter, *Coherence and Time Delay Estimation*. New York: IEEE Press, 1993.

[30] A. Weiss and E. Weinstein, "Fundamental limitations in passive time-delay estimation-Part I: Narrowband systems," *IEEE Trans. Acoust., Speech, Signal Processing*, vol. ASSP-31, pp. 472–486, Apr. 1983.

K. C. Ho (S'89–M'91–SM'00) was born in Hong Kong. He received the B.Sc. degree with First-Class Honors in electronics and the Ph.D. degree in electronic engineering from the Chinese University of Hong Kong in 1988 and 1991, respectively.

He was a research associate in the Department of Electrical and Computer Engineering, Royal Military College of Canada, Ottawa, ON, Canada, from 1991 to 1994. He joined Bell-Northern Research, Ottawa, in 1995 as a member of scientific staff. He was a faculty in the Department of Electrical Engineering, University of Saskatchewan, Saskatoon, SK, Canada from September 1996 to August 1997. Since September 1997, he has been with the University of Missouri-Columbia, where he is currently an Associate Professor with the Electrical and Computer Engineering Department. He is also an Adjunct Associate Professor at the Royal Military College of Canada. His research interests are in statistical signal processing, landmine detection, source localization, wavelet transform, wireless communications, and the development of efficient adaptive signal processing algorithms for various applications including landmine detection, echo cancellation, and time delay estimation. He has been active in the development of the *ITU Standard Recommendation G.168: Digital Network Echo Cancellers* since 1995. He is the editor of the *ITU Standard Recommendation G.168*. He has three patents from the United States in the area of telecommunications.

Dr. Ho was the recipient of the Croucher Foundation Studentship from 1988 to 1991 and received the Junior Faculty Research Award from College of Engineering of the University of Missouri-Columbia in 2003. He is an Associate Editor of the IEEE TRANSACTIONS ON SIGNAL PROCESSING and the IEEE SIGNAL PROCESSING LETTERS.

Wenwei Xu (M'01) was born in Shanghai, China. He received the B.S. degree in mechanical engineering from Shanghai Maritime University in 1991 and the M.S. degree in electrical engineering in 2001 and the Ph.D. degree in mechanical and aerospace engineering in 2002, both from the University of Missouri-Columbia.

He was an engineer at the Waterborne Transportation Institute, Ministry of Communications of P.R. China, Beijing, China, from 1991 to 1994. He joined Lucent Technologies as a member of technical staff in 2001. Currently, he is as a consulting engineer for Legato Video, LLC, NJ. His research interests include digital signal processing, real-time control, system modeling, and telecommunications.

Dr. Xu received Donald Anderson Teaching Award from University of Missouri-Columbia in 2000.